Micromechanical Study on Moisture Induced Tensile Strength Reduction of GFRP

*GAO Chaogan, ZHOU Chuwei**

State Key Laboratory of Mechanics and Control of Mechanical Structures, Nanjing University of Aeronautics and Astronautics, Nanjing 210016, P.R. China

(Received 30 April 2020; revised 3 July 2020; accepted 20 January 2021)

Abstract: The main focus of this paper is to investigate the influence of hygrothermal aging on tensile strength of epoxy resin matrix composites. Firstly, tests of water absorption and moisture induced tensile strength degradation of glass fiber reinforced polymer (GFRP) are conducted. Results show that the moisture absorption behavior of the GFRP follows the Fick's law, and its tensile strength retention decreases notably in the early hygrothermal aging stage and then gradually approaches a constant. Then, microscale longitudinal and transverse strength prediction models for unidirectional fiber reinforced composites are proposed. They are moisture concentration dependent and reflect the inherent probability of failures of fiber and matrix (or fiber/matrix interface). The moisture diffusing analysis demostrates that the proposed models can predict degradation of tensile strength of epoxy resin matrix composites undergoing different hygrothermal durations. The proposed models are validated by the experiments of hygrothermal residual strength of the GFRP mentioned above.

Key words: composites; hygrothermal aging; residual strength; micromechanics; probability model

CLC number: TB332 **Document code:** A **Article ID:** 1005-1120(2022)02-0250-13

0 Introduction

Fiber reinforced polymer composites (FRPs) have high specific strength and stiffness, as well as superior performances on fatigue and corrosion resistances. Attributing to these advances as well as the cost reduction and forming process improvement, FRPs have been growingly employed in marine structures and shipbuilding structures nowadays[1]. Modern ships need lighter structures to carry more goods or equipment, and the designability of FRP can combine structural and some functional needs together to save space in the ship. All these needs make composites one of the most attractive candidate materials in ship design[2]. FRPs have been widely used in superstructures and hull structures of modern yachts, and they have been increasingly applied to even navy ships in recent years[3]. However, one of the challenges in the application of epoxy matrix composites in marine and ship structures is their duration properties in hygrothermal environment. High moisture, ultraviolet radiation and temperature variation might cause severe property reduction for polymer materials. Therefore, the long term mechanical behaviors of FRP should be well assessed to ensure they have sufficient residual strength in their server lives[4-5].

Experimental test is the direct and the most reliable way to study the aging characteristics of composite materials, and a great amount of relevant research work has been reported in the literature. Among them, the property degradation of glass fiber reinforced polymer (GFRP) under different humidity and temperature conditions has been studied extensively[4-13]. These studies have proven that temperature and humidity are the two major environment factors on aging of GFRP[14]. The experimental studies are classified into two catagories in gener-

*Corresponding author, E-mail address: zcw@nuaa.edu.cn.

How to cite this article: GAO Chaogan, ZHOU Chuwei. Micromechanical study on moisture induced tensile strength reduction of GFRP[J]. Transactions of Nanjing University of Aeronautics and Astronautics, 2022, 39(2): 250-262.

http://dx.doi.org/10.16356/j.1005-1120.2022.02.011

al, i.e., tests of mechanical properties and physical (or chemical) properties. The former includes stiffness and strength tests of GFRP under various stress conditions. And the often used tests of the latter include measurement of glass transition temperature (T_g) by dynamic mechanical analysis(DMA) or differential scanning calorimetry(DSC)[15], observation of morphologies on surface or fracture cross section by scanning electron microscopy(SEM)[5-6,8], and detecting crosslinking change of polymer chain by nuclear magnetic resonance technique(NMR)[16]. From Refs.[14-16]it can be found that both the properties in these two catagories can be affected significantly by hygrothermal environment. For instance, the tensile strength and modulus of GFRP might degrade 29% and 23%[5] after hygrothermal aging and meanwhile its T_g decreases 3 ℃[15]. SEM observations show that hygrothermal aging promotes micro crack occurrence at the fiber/matrix interface[5-6], and this phenomenon translates the mechanism of mechanical aging. It can be concluded that the main contributions of the hygrothermal aging to composites are: (1) The property degradations of component phases, for example, water absorption might plasticize, soften or even hydrolyze the epoxy resin matrix phase; (2) thermal and moisture mismatch deformations. Mismatching deformations introduce residual internal stress which might cause irreversible damages such as crazing and micro cracks in matrix and debonding at the fiber/matrix interface[17-18].

Tensile property is one of the basic mechanical parameters of composites concerned in structure and material design. The load carrying ways and tensile failure mechanisms of unidirectional composite (UD) under longitudinal and transverse tensions are quite different, which leads to the big gaps between strength and critical elongation rate for UD under 0° and 90° directions. Fibers bear most of the load under the longitudinal tension, therefore the tensile strength of 0° UD mainly depends on that of fibers. The tensile strengths of fibers are not identical and they usually fail gradually under the tensile load. The broken fiber does not carry load at the fracture, but the shear force transmitted through the fiber wrapping matrix gradually recovers the load at a position far from the fracture. Tensile strength distribution of fibers is often considered in the shear lag model which can well represent the damage mechanism of UD under tensions[19-20]. The failure mechanism of UD under the transverse tension is the micro cracks nucleate in matrix or at the fiber/matrix interface and then propagates and coalesces to a critical main crack. The strengths of the matrix and fiber/matrix interface as well as fiber volume fraction and fiber aggregation can all affect UD transverse strength, so microscopic finite element methods are often employed to describe transverse tensile strength of UD[21-22]. Under the aging damage of the composites in a humid and hot environment, the matrix and the fiber/matrix interface will be affected by hydrolysis and residual stress, which finally reduces the composite strengths (especially for the transverse and the shear strength) obviously. A hygrothermal damage model is desired to represent the dominant hygrothermal aging mechanism and the model parameters can be calibrated through limit experiments. Unfortunately, current residual tensile strength evaluation methods for composites experienced hygrothermal aging are basically mathematical fitting of aging data[10,16,20,23-24], which means that the aging curve obtained by fitting a composite test specimen is not applicable to the composites with different layers or different aging environments.

This paper aims to establish a quantitative relationship between tensile properties and moisture absorption of composite materials, and to predict the residual strengths of composites under different moisture absorption conditions. Firstly, moisture absorption behaviors of GFPR in the hygrothermal condition are experimentally studied. Secondly, the residual tensile strength prediction models of 0° UD and 90° UD are established. Finally, the models are evaluated through hygrothermal aging experiment results.

1 Experimental Study

1.1 Preparation of composite specimens

The glass fiber used in unidirectional and or-

thogonal composites was produced by Nanjing Glass Fiber Research Institute. Its item number was EWU210-100 and area density was 200 g/m^2. The matrix was epoxy resin produced by East China University of Science and Technology, and its item number was MERICAN30-200P. The curing agent was PROMOX P200TX produced by Sino Composite, and the promoter was octylic acid cobalt salt. The tensile strength and modulus of the matrix material were measured as 95 MPa and 3.4 GPa, respectively, from the bulk epoxy specimen made by casting molding.

The unidirectional E-glass fiber reinforced composite specimen was prepared by vacuum infusion process (VIP), and the air pressure used was 0.1 MPa. The mass ratio of resin, curing agent and promoter was about 100∶1∶1. The environment temperature was kept at 25 ℃ and humidity below 60% RH during the blending of resin and vacuum conductivity process. The mass ratios of curing agent and promoter for specimens of different batches might be finely adjusted in order to let resin fully infiltrate the fiber cloth in VIP. The ply number of UD and orthogonal specimens were $(0^\circ)_{12}$ and $(0^\circ/90^\circ)_{4s}$, respectively. The specimens were then placed in a drying oven (50 ℃) for 24 h to cure completely. VIP and the three kinds of specimens are shown in Fig.1 and Fig.2. The cured plates of unidirectional and orthogonal composites were 2.24 mm and 2.88 mm in thickness with glass fiber volume content of 42.18% and 43.74%, respectively.

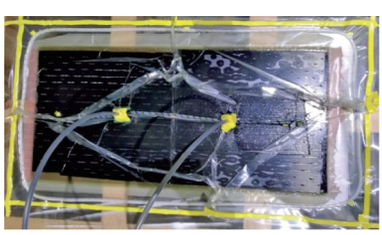

Fig.1 Vacuum infusion process

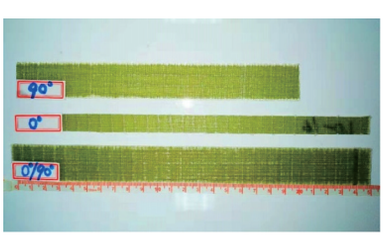

Fig.2 Three kinds of specimens

1.2 Experiment of hygrothermal aging

The prepared specimens were exposed in the humidity test chamber for 1, 3, 6, 10 and 15 d. The temperature in the test chamber was 60 ℃ and the relative humidity was 95%. Before hygrothermal aging tests, all the specimens were put in the drying oven at 50 ℃ for 24 h for drying up and curing completely. Then the initial dry mass of all test pieces was measured by electronic balance of Mettler Toledo AL-104. The lateral surfaces of all specimens were coated by waterproof coating to avoid edge effect.

During the hygrothermal aging experiment, water gain of each specimen was measured with regular intervals according to ASTM D5229[25]. The number of each kind of specimens is 5 in one test. Before weighing, the liquid water on the surface of each specimen was dehumidified with absorbent paper. The weight gain percentage of the moisture content of the specimen is calculated by the following equation

$$W_t = \left(100 \times \frac{M_t - M_0}{M_0}\right)\% \tag{1}$$

where M_0 and M_t are the mass of specimens at the initial dry state and after exposed in the humidity test chamber for time of t.

1.3 Experiment of tensile strength

Tension experiments of GRFP experiencing hygrothermal aging durations for 1, 3, 6, 10 and 15 d were conducted. 0° UD and 90°UD specimens were cut from the UD plate along and vertical to the fiber direction by a water jet scalpel, and 0°/90° specimens were cut from the 0°/90°orthogonal composite plate. Friction tabs made of 6061 aluminum alloy were bonded at both ends of these specimens, as shown in Fig.3, where L_T is the length of aluminum alloy tab, L_G the length of test section, h_G the thickness of test section, h_T the thickness of tab,

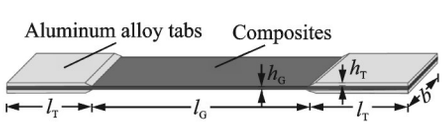

Fig.3 Specimen schematic of GFRP tensile test

and b the width of specimen. And the dimensions of these composite specimens were listed in Table 1. Tensile moduli and strengths of the three kinds of specimens were tested at the initial dry state and after hygrothermal aging. Specimens were taken out from humidity test chamber for tensile tests after 1, 3, 6, 10 and 15 d. In order to eliminate the effect of experiment data dispersion, at least five effective samples were used for each experiment group[26]. The experimental apparatus was the INSTRON2360 universal testing system with the load capacity of 50 kN. The tensile test speed was kept at 2 mm/min, and the room temperature was controlled at 20 ℃±5 ℃.

Table 1 Dimensions of tensile specimens mm

Fiber orientation	Width	Overall length	Thickness	Tab length	Tab thickness
0° UD	12.5	250	2.20	50	1.5
90° UD	25	200	2.20	25	1.5
0°/90° cross-ply	25	250	2.88	50	1.5

2 Probabilistic Tensile Strength Modeling of UD

2.1 Distributions of moisture concentration and corresponding tensile strength

Infiltrated moisture in polymer matrix composites might damage its microstructures chemically or/ and mechanically, thus it leads to property degradation of composites. So the moisture concentration is one of dominations in hygrothermal aging of composites. Moisture concentration does not uniformly distribute in composites before it has achieved saturation. A refined hygrothermal aging study should consider this unevenness of moisture concentration in composites. Moisture diffusion in composites has been proven to follow the Fick's second law in general[27]. One-dimensional Fick's second law is expressed as

$$\frac{\partial c}{\partial t}=D\frac{\partial^2 c}{\partial x^2} \tag{2}$$

where c is the moisture concentration, D the diffusion coefficient, and x the coordinate along the diffusion direction. By the uniform moisture boundary condition, the time dependent concentration distribution can be derived from Eq.(2) as

$$c(x,t)=c_0\left(1-\frac{4}{\pi}\sum_{k=1}^{\infty}\frac{1}{2k-1}\sin\frac{(2k-1)\pi}{h}x\cdot e^{-\frac{(2k-1)^2\pi^2 Dt}{h^2}}\right) \tag{3}$$

where c_0 is the saturation concentration, and h the interval of the two moisture surfaces, i.e., the thickness of a composite plate in this study.

The weight gain expression of one-dimensional diffusion can be obtained by integrating the concentration $c(x,t)$ in the thickness direction, that is

$$M(t)=c_0 h\left(1-\frac{8}{\pi^2}\sum_{k=1}^{\infty}\frac{1}{(2k-1)^2}\cdot e^{-\frac{(2k-1)^2\pi^2 Dt}{h^2}}\right) \tag{4}$$

It has been experimentally proven that water absorption directly leads to the decrease in composite strength[20,23,28-30]. Here if the strength of a composite is expressed as a function of moisture concentration, for one diffusion case the average residual tensile strength of the composite laminate is obtained via integrating strength of each infinitesimal layer along thickness, shown as

$$S(t)=\frac{1}{h}\cdot\int_{-h/2}^{h/2}\sigma(c(x,t))\mathrm{d}x \tag{5}$$

where σ is the moisture dependent tensile strength of the composite and thus also the function of coordinate x and moisture duration time t.

If Eq.(5) is not analytically integrable, the integration can be alternated by numerical summation. For example, a composite laminate is discretized to numbers of uniform thick layers, as illustrated in Fig.4(a), and the continuous distributions of moisture, as well as residual strength along thickness, are simplified as stair shaped broken lines (Figs.4(b,c)). In other words, the moisture concentration and strength in one layer are homogenized. In this way, the average strength of a composite laminate is expressed as

$$S(t)=\frac{1}{h}\cdot\sum_{i=1}^{n}\sigma(\bar{c}_i(x_i,t))\cdot h_i \tag{6}$$

$$\bar{c}_i(x_i,t)=\frac{1}{h_i}\int_{x_i}^{x_i+h_i}c(\xi,t)\mathrm{d}\xi \tag{7}$$

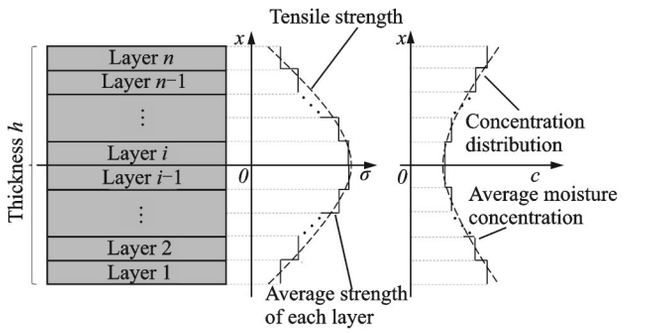

(a) Schematic of laminate (b) Strength distribution (c) Moisture distribution

Fig.4 Schematic of stagewise average strength method

where $\bar{c}_i$ and h_i are the average moisture concentration and the thickness of the ith layer, respectively; n is the total number of layer discretization and if it is large enough the summation of Eq.(6) will approach the exact integration value with sufficient accuracy.

2.2 Longitudinal tensile strength model of UD

Experiments have proven that the tensile strength of glass fibers agrees with the Weibull distribution[31-32]. Under the longitudinal tension, fibers in UD break from the weakest one to the strongest one step by step instead of breaking simultaneously. A broken fiber will unload completely at the fracture point, but the surrounding matrix may gradually transmit tensile loads to the broken fiber through the shear stress over a length, thus the residual tensile stress will increase from zero to an intact value in a certain length. This stress recovery length, named L_{Lr} here, is the so-called "ineffective length", one of the key parameters determining the ultimate longitudinal tensile failure stress[33-34], and its value depends on the tensile load applied[19].

In this paper, a micromechanical strength model is proposed based on the idea of modified stress transfer "shear-lag" model[19-20,35]. As illustrated schematically in Fig.5(b), a rectangular region with a length of L_{Lr} in UD is taken as the longitudinal representative volume element (LRVE) for modeling tensile strength prediction. The main relevant assumptions made for LRVE are:

(1) LRVE contains enough fibers to reflect the strength distribution. Meanwhile, it is small enough to be viewed as a point in UD.

(2) For the break density saturation of fibers, we assume one fiber has one broken point at most in LRVE[32].

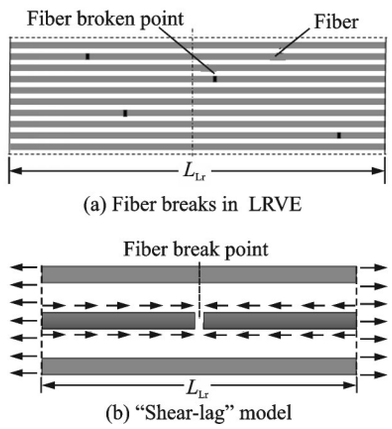

Fig.5 Schematic of fiber breaks in LRVE and "shear-lag" model

(3) The possible position of the broken point for a fiber distributes evenly in a LRVE scope, and the possibility of two or more adjacent fibers breaking at the same cross section is not considered[19].

(4) Fiber packing is idealized as hexagonal pattern as shown in Fig.6.

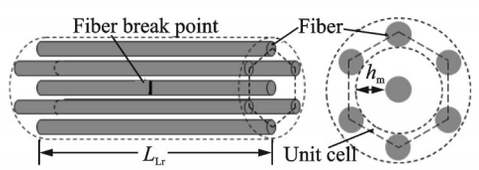

Fig.6 Idealized hexagonal packing of fibers

For the force equilibrium consideration, the average tensile stress of any cross section for LRVE is identical and equals the tensile stress. To the middle cross section of LRVE, the possibilities of broken points of fibers locating in its left and right sides are

equal in average, and the average locations of broken points in the two sides are all $L_{Lr}/4$ away from the center cross section. The average tensile stress of the middle cross section of LRVE is the quantitative mixture of tensile stresses of broken and unbroken fibers, expressed as[19]

$$\sigma_{fa}(t)=\sigma_{f0}[1-P(\sigma_{f0})]+P(\sigma_{f0})\sigma_{fb}(L_{Lr}/4) \quad (8)$$

where σ_{f0} and σ_{fb} are the stresses on the unbroken and the broken fibers, respectively; P is the cumulative probability of fracture fibers and depends on tensile load σ_{f0}, hence depends on ineffective length L_{Lr}. It can be estimated by the following equation[31]

$$P(\sigma_{f0})=1-\exp\left[-L_{Lr}\left(\frac{\sigma_{f0}}{\sigma_{Lr}}\right)^{\rho_L}\right] \quad (9)$$

where the model parameters σ_{Lr} and ρ_L are named characteristic strength and Weibull modulus, and they can be fitted from the tensile experiment of single fiber specimen. In practical specimens with a much larger gauge length ($L_L \gg L_{Lr}$) are usually used to measure the probability of fiber fracture for feasibility. The probability estimation of fiber breakage transfers to an equivalent form Eq.(10)[31], which involves practical gauge length L_L.

$$P(\sigma_{f0})=1-\exp\left[-\frac{L_{Lr}^2}{L_L}\left(\frac{\sigma_{f0}}{\sigma_L}\right)^{\rho_L}\right] \quad (10)$$

From Eq.(8) and Eq.(10), we can see that stress recovery length L_{Lr} is one of the dominant factors determining the tensile strength of load carry capacity of the composite. L_{Lr} can be estimated by the global load sharing (GLS) model[35-36]. In this model a broken fiber is assumed surrounded by six fibers and the broken points for the surrounding fibers (if exist) are beyond scope of L_{Lr}. L_{Lr} is assumed to be dependent on the remote tensile stress (also the tensile stress for the unbroken fiber σ_{f0}) by Morais[35], defined as

$$L_{Lr}=\frac{d_f\sigma_{f0}}{4\tau_{pm}}-\frac{1}{\beta}\left\{1+\ln\left[\frac{(1-\alpha)d_f\sigma_{f0}}{4\tau_{pm}}\right]\right\} \quad (11)$$

$$\beta=\sqrt{\frac{4G_m}{d_f h_m E_f}} \quad (12)$$

where d_f is the diameter of a fiber; τ_{pm} is the yield shearing stress of the fiber/matrix interface; G_m and E_f are the matrix shear modulus and the fiber longitudinal modulus, respectively; Parameter α, named high fraction, is the ratio of the recovered tensile stress to the tensile stress in an unbroken fiber σ_{f0}, and in practical calculation α can take a value close to 1 but less than 1; h_m is the average separation of a fiber to the adjacent fibers. As shown in Fig.6, it can be calculated through the fiber volume fraction V_f, shown as

$$h_m=d_f\left(\sqrt{\frac{\sqrt{3}\,\pi}{6V_f}}-1\right) \quad (13)$$

It is worth noticing that the above equations are also reasonable approximations for the interface debonding case at fiber broken area[35]. When the value of recovery length L_r is determined, the ultimate tensile strength of a composite is defined as the maximum tensile stress it can bear, so it is the extreme value of σ_{fa}, shown as

$$\frac{d\sigma_{fa}}{d\sigma_{f0}}=0 \quad (14)$$

Eq.(14) is an implicit function of variable σ_{f0} and Morais[19] gave a closed-form solution with some simplifying assumptions that

$$\sigma_{ut0}=\left[\frac{16(\tau_{pm})^2 L_L \sigma_L^{\rho_L}}{(\rho_L+2)d_f^2}\right]^{\frac{1}{\rho_L+2}}\exp\left(-\frac{1}{\rho_L+2}\right) \quad (15)$$

where τ_{pm} is considered to be weaken by moisture infiltration. Pritchard et al.[21] proposed an exponential form of τ_{pm} through fitting a large number of experimental data and it degrades with moisture concentration. Here we used a two-order polynomial function to describe the moisture affected fiber/matrix interfacial yield shear stress, shown as

$$\tau_{pm}=\tau_0+\tau_1\bar{c}+\tau_2\bar{c}^2 \quad (16)$$

where τ_0, τ_1 and τ_2 are empirical constants. The tensile strength in one point of the composite is calculated from the mixtures law as

$$s_0=V_f\sigma_{ut}+(1-V_f)\sigma_m\approx V_f\sigma_{ut} \quad (17)$$

where σ_m is the ultimate strength of the matrix. Submitting Eq.(16) and Eq.(17) to Eq.(6), the residual tensile strength of UD in 0° direction is expressed as

$$S_0(t)=\frac{V_f}{h}\cdot\left\{\frac{16[\tau_0+\tau_1\bar{c}_t^i+\tau_2(\bar{c}_t^i)^2]^2 L_L\sigma_L^{\rho_L}}{(\rho_L+2)d_f^2}\right\}^{\frac{1}{\rho_L+2}}\cdot \exp\left(-\frac{1}{\rho_L+2}\right)\cdot h_i \quad (18)$$

2.3 Transverse tensile strength model of UD

Hygrothermal environment significantly affects transverse strength of UD, which has been proven by numerous experiments[14-15,21]. Addition to empirical formula, micro finite element simulations were often employed to evaluate transverse strength of UD in hygrothermal environment. These numerical approaches can well represent evolutions of multi damages such as local matrix failures and fiber/matrix interface debonding[22]. However, they are usually time-consuming for modeling and computing. Here, we extend the idea of longitudinal tensile strength LRVE model to transverse strength prediction of UD. As shown in Fig.7(a), fibers in UD are idealized hexagonal arrangement and a debonding fiber is simplified as a void. This implies that all the interface damages are assumed full interface debonding.

From Fig.7(a) we can see that a rectangular shape of representative volume element (RVE) for transverse property investigation of UD is chosen (transverse representative volume element, named TRVE in this paper). TRVE is viewed as a point in UD. It includes enough fibers to characterize the randomness of the fiber/matrix interface debonding and matrix failures in micro-view. TRVE can be subdivided to several uniform thickness tapes and each tape contains one layer fibers with an uniform interval. One tape is also viewed as a chain of fibers connected by matrix, named fiber-matrix chains (FMC) in series. The assumptions imposed on TRVE, similar to those on LRVE, include: (1) No initial matrix damage exists in TRVE; (2) one FMC has one interface failed fiber (IFF) at most; (3) the possible position of IFF distributes evenly in a TRVE scope, and the possibility that two or more adjacent FMCs have IFFs at the same cross section is not considered.

FMCs in TRVE can be analogous to longitudinal fibers in LRVE, and an IFF in TRVE can be analogous to a broken point of fibers in LRVE. In local region of IFF, the tensile stress diminishes greatly. It bypasses this region and then reloads on FMC gradually over a length. The unloading and reloading of the tensile stress are simulated by the analytical approach[37]. As shown in Fig.7(b), IFF is simplified as a circle void and the heterogenous material around is homogenized as homogenous isotropic medium. Under the far filed tension, the tensile stress distribution along the line through the void center is calculated as[37]

$$\sigma_{md}(x)=\sigma_{m90}\left(1-\frac{5}{32}\frac{{d_f}^2}{x^2}+\frac{3}{128}\frac{{d_f}^4}{x^4}\right)$$
$$\frac{1}{2}d_f\leqslant x\leqslant\infty \tag{19}$$

where σ_{md} and σ_{m90} are the tensile stresses in broken and unbroken FMCs, respectively. Tensile stress is 0 at IFF edge ($x=\pm 0.5d_f$) and it increases with the distance x going far away from the IFF region. Parameter L_{Tr} is the distance where the tensile stress recovers 95% of the value of FMC without IFF. From Eq.(19) the recovery length L_{Tr} is obtained about $3.5d_f$. The tensile stress distribution along the central line of FMC with IFF is demonstrated in Fig.7(b). The transverse tensile stress recovery length L_{Tr} can be analogous to the ineffective length L_{Lr} defined in LRVE, and it is also used as the length of TRVE.

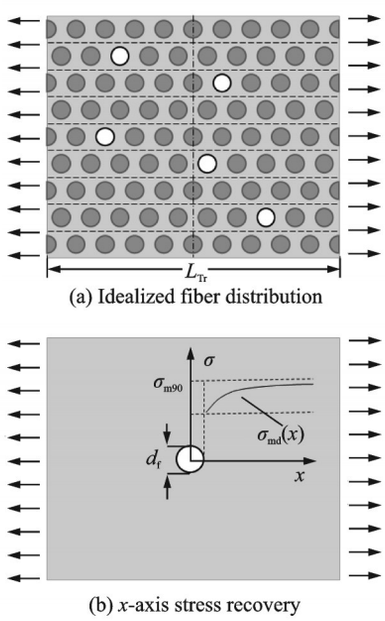

Fig.7 Schematic of fiber/matrix interface debonding in the RVE of 90° UD composites

The central cross section of TRVE is chosen to calculate the average tensile stress in TRVE. With the assumptions suggested in this section, the numbers of IFFs locating at both sides are con-

sidered the same and their average positions are at the middle of these two halves of TRVE. Thus the average tensile stress in TRVE is weighted by possibilities of tapes with and without IFF, shown as

$$\bar{\sigma}_{ma} = \sigma_{m90}[1 - P(\sigma_{m90})] + P(\sigma_{m90})\sigma_{md}(L_{Tr}/4) \quad (20)$$

where $\bar{\sigma}_{ma}$ is the average stress and $P(\sigma_{m90})$ the cumulative probability of interface debonding of the fiber, shown as[31]

$$P(\sigma_{m90}) = 1 - \exp\left[-L_{Tr}\left(\frac{\sigma_{m90}}{\sigma_{Tr}}\right)^{\rho_T}\right] \quad (21)$$

where σ_{Tr} is a characteristic strength of FMC corresponding to length L_{Tr}; and ρ_T is the Weibull modulus. If the transverse tensile strength of UD is obtained from the experiment (or from the micromechanical simulation) with an observation length (or a micromechanical model length) L_T which is usually much larger than L_{Tr}, the probability of fiber interface debonding of Eq.(21) can be rewritten though analogizing the LRVE model, as

$$P(\sigma_{m90}) = 1 - \exp\left[-\frac{L_{Tr}^2}{L_T}\left(\frac{\sigma_{m90}}{\sigma_T}\right)^{\rho_T}\right] \quad (22)$$

It is worth noting that the strength of FMC is not constant, and it changes synchronously with its moisture concentration. Here shape parameter ρ_T in Eq.(21) and Eq.(22) is assumed invariable while strength parameter σ_T as quadratic polynomial equation of moisture concentration, shown as

$$\sigma_T = \sigma_0 + \sigma_1\bar{c} + \sigma_2\bar{c}^2 \quad (23)$$

where σ_0 is the strength of FMC in the dry state; σ_1 and σ_2 are empirical constants employed to fit the strength of FMC in the humid state.

The tensile strength of UD which is defined as the maximum tensile load carrying capacity of TRVE is obtained by solving Eq.(24).

$$\frac{d\bar{\sigma}_{ma}}{d\sigma_{m90}} = 0 \quad (24)$$

Using the simplified assumptions proposed by Morais[19], we can obtain the critical tensile stress from Eq.(24), shown as

$$\sigma_{ut90} = \sigma_T\left(\frac{L_T}{\rho_T L_{Tr}^2}\right)^{\frac{1}{\rho_T}} \quad (25)$$

By submitting Eqs.(22, 23, 25) to Eq.(20), the average ultimate strength in the ith layer of 90° UD can be obtained, shown as

$$\sigma_{ut90}^i = \left[0.66 + 0.34\cdot\exp\left(-\frac{1}{\rho_T}\right)\right]\left(\frac{L_T}{\rho_T L_{Tr}^2}\right)^{\frac{1}{\rho_T}}\cdot[\sigma_0 + \sigma_1\bar{c}^i + \sigma_2(\bar{c}^i)^2] \quad (26)$$

The expression of the residual tensile strength of 90° UD is

$$S_{90}(t) = \frac{1}{h}\cdot\sum_{i=1}^{n}\sigma_{ut90}^i\cdot h_i \quad (27)$$

The fracture strain of 0° UD is much larger than that of 90° UD, which means that the 90° plies fail before the 0° plies in the orthogonal composite under the uniaxial tensile load. The cracked 90° plies cohere to the 0° plies except in the crack region where delamination usually occurs. So cracked 90° plies can still have some residual load carrying capacity before the ultimate failure of the orthogonal composite. Here, two extreme cases are assumed:

(1) 90° plies and cracked 0° plies in the orthogonal composite fail synchronously, which means the tensile strength of the orthogonal composite is the volume weight average of tensile strengths of 0° plies and 90° plies.

(2) All 90° plies have failed when 0° plies begin to fracture in the orthogonal composite, in other words, contributions to the tensile strength of the orthogonal composite from 90° plies are ignored.

The ultimate strength of the orthogonal composite is expressed as

$$S_{090}(t) = \frac{1}{h}\cdot\sum_{i=1}^{n}\bar{\sigma}^i(c^i(t))\cdot h_i \quad (28)$$

For Case 1

$$\bar{\sigma}^i(c^i(t)) = \begin{cases}\sigma_{ut0}^i & \text{When the } i\text{th layer is } 0^\circ \text{ ply}\\ \sigma_{ut90}^i & \text{When the } i\text{th layer is } 90^\circ \text{ ply}\end{cases} \quad (29)$$

For Case 2

$$\bar{\sigma}^i(c^i(t)) = \begin{cases}\sigma_{ut0}^i & \text{When the } i\text{th layer is } 0^\circ \text{ ply}\\ 0 & \text{When the } i\text{th layer is } 90^\circ \text{ ply}\end{cases} \quad (30)$$

The expressions of σ_{ut0}^i and σ_{ut90}^i are defined in Eq.(15) and Eq.(26), respectively. It can be seen that Case 1 overestimates the ultimate tensile strength of the orthogonal composite, while Case 2 underestimates it. The deviations between these two cases will be discussed in the next section.

3 Results and Discussion

3.1 Moisture absorption experiment

Water absorption experiment of the GFRP was conducted and the result is shown in Fig.8. It can be found that the weight gain curves of 0° UD, 90° UD and orthogonal composite specimens all follow the Fick's law. The diffusivity coefficients and moisture saturation ratios of these three kinds of specimens are measured almost the same, and they are 0.008 1 mm^2/h and 0.47%, respectively. It is noticed that, for 0° UD the long side surface is along the fiber direction and the short side surface is transverse to the fiber direction; for 90° UD the situation is opposite. Since these two kinds of lateral surfaces have different water diffusivities, the identification of the weight gain curves for 0° and 90° UDs, as shown in Fig. 8, indicates that the waterproof coatings of specimens have good effect. Therefore, moisture absorptions of these specimens can be treated reasonably as one-dimensional diffusion problem.

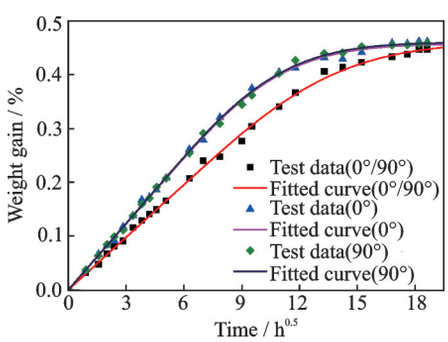

Fig.8 Weight gain curves of three kinds of specimens

3.2 Tensile strength experiment

Tensile experiments were conducted on the unidirectional and orthogonal GFRPs to determine GFRP's residual strengths at different hygrothermal aging durations. The stress-strain curves of the three kinds of specimens after various ageing times are shown in Figs.9—11. The corresponding tensile strength retentions are listed in Table 2.

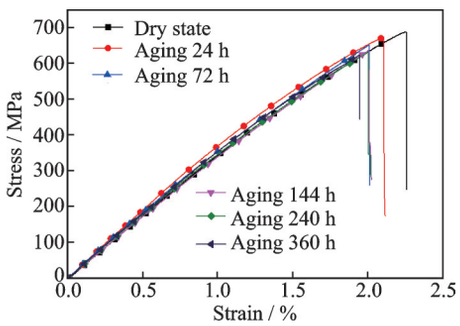

Fig.9 σ-ε curves of 0° GFRP after aging

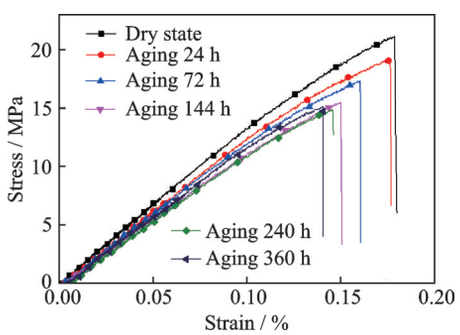

Fig.10 σ-ε curves of 90° GFRP after aging

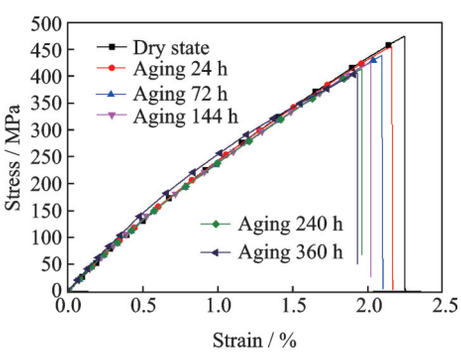

Fig.11 σ-ε curves of 0°/90° GFRP after aging

Table 2 Tensile strength retention rate of three kinds of composites after hygrothermal aging

Aging time/h	0° UD GFRP		90° UD GFRP		0°/90° GFRP	
	Average strength/MPa	Retention rate/%	Average strength/MPa	Retention rate/%	Average strength/MPa	Retention rate/%
0	687.54	100.00	21.07	100.00	471.89	100.00
24	670.18	97.48	19.13	90.79	453.97	96.20
72	651.32	94.73	17.29	82.06	437.19	92.65
144	637.14	92.67	15.43	73.23	424.27	89.91
240	632.36	91.97	14.83	70.38	412.45	87.40
360	630.02	91.63	14.68	69.67	404.02	85.62

3.3 Tensile strength prediction

The yield shearing stress of the fiber/matrix interface is difficult to directly measure by experiments, especially in the wet state. For MERICAN30-200P epoxy matrix, the tensile strength, modulus and Poisson's ratio were 90 MPa, 3.4 GPa and 0.42, respectively in the dry state provided by the supplier. If using the von Mises stress to determine the failure of matrix materials, the quantity of the shear strength will be 0.6 times of the tensile one. But some researchers pointed out that polymers underwent tensile failures in shear tests[38-39]. In this viewpoint, τ_{pm} should be equal to the yield tensile stress. For EWU210-100 E-glass fiber, the Weibull modulus ρ_L and characteristic strength σ_L at a 15 mm characteristic length were 9.88 and 1 000 MPa, respectively, provided by the supplier. The diameter of the glass fiber was 10 μm. The tensile strength prediction for 0° UD at any moisture state has three undetermined parameters of τ_0, τ_1 and τ_2. They were calibrated by the least square fitting the tensile strength tests under different moisture states. The initial values of these undetermined parameters have some effects on the final fitted values. So here the value of τ_0 was chosen 90 MPa and 54 MPa, and τ_1 and τ_2 accordingly were chosen 200 times and 40 000 times of the quantity of τ_0, respectively, to let the second and the third terms in the right side of Eq.(16) keep the same order of magnitude with the first term. The multiplier of τ_1 and τ_2 was close to the reciprocal and square reciprocal of the saturate moisture concentration of these composites. It was found that when the original τ_0 was chosen as 54 MPa (0.6 times of the dry tensile strength of matrix materials), the fitted curve well met the experimental data, and the final fitted values were 55.01, -4.55×10^4 and -3.44×10^7 MPa. It is noticeable that the final fitted τ_0 was quite close to the von Mises strength of matrix material in dry state. The experimental and predicted residual tensile strength of 0° UD GFRP are shown in Fig.12.

The transverse strength of UD is dominated by those of the matrix and fiber/matrix interface. To the microscale transverse tensile strength model proposed in this paper, the strength distribution parameters of FMCs in TRVE in dry state are difficult to measure directly in practical tests. Here, they were substituted by the strength distribution parameters of 90° UD specimens in the dry state. The Weibull modulus ρ_T and the initial value of the characteristic strength σ_T at characteristic length L_T for 90° UD specimens were fitted as 29.16 and 21.01 MPa, respectively, and they were assumed also real to the FMC. Similarly, the empirical parameters for characteristic strength σ_T, i.e., σ_0, σ_1 and σ_2 were calibrated by fitting Eq.(27) with experimental strength ageing data of 90° UD. Here, initial value of σ_0 was chosen as the tensile strength of 90° UD, and the initial values of σ_1 and σ_2 accordingly were chosen as the 200 times and 40 000 times of quantity of σ_0, respectively, with the similar reason for 0° UD situation. Through the least square fitting, they were 21.01, $-2\ 766.72$ and -3.61×10^7 MPa, respectively. The predicted residual tensile strength curve of 90° UD GFRP is also shown in Fig.12. It can be seen that the strength of the 90° UD GFRP decreases more sharply after hygrothermal aging than those of the two other specimens.

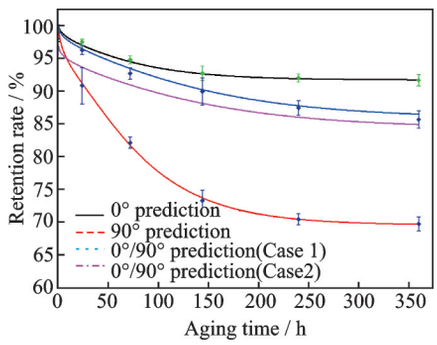

Fig.12 Residual tensile strength predictions of GFRPs undergoing hygrothermal aging

When the residual tensile strength prediction models of 0° UD and 90° UD GFRP have been built, the upper and lower bounds for residual tensile strength of 0°/90° GFRP can be predicted by Eq.(28), and the results are shown in Fig.12. As we can see from Fig.12, the predicted results of Case 1 slightly overestimates the residual strength of the orthogonal composite, because it assumes the

0° and 90° plies fail synchronously. This case usually does not occur on real composites. The predicted results of Case 2 underestimates the residual strength, especially in the early stages of aging, because in this case the contribution of 90° layers to the tensile strength is ignored completely and this assumption is also not real. It is noticed that Case 1 gives better prediction than Case 2, since the humidity affects the transverse tensile strength more than it does on the longitudinal tensile strength. The predicted curve of Case 2 is close to that of Case 1 with aging time increasing. More specifically, the largest discrepancy of the predicted upper and lower residual tensile strength are only 2.97%.

4 Conclusions

This paper investigated the tensile strength degradation of GFRP during hygrothermal aging. Unidirectional and cross-ply EWU210-100 glass/vinyl ester resin composites were made, and experiments of water absorption and residual tensile strength after different water update durations were conducted. Microscale longitudinal and transverse tensile strength models for UD were proposed. The main conclusions of this study are as follows:

(1) The moisture absorption of this GFRP follows the Fickian behavior. The diffusivity coefficients and moisture saturation ratios of all three kinds of specimens of this GFRP are almost the same as 0.008 1 mm^2/h and 0.47%, respectively. In other words, the specimens of this composite with different ply patterns have the same moisture diffusion characteristics if they possess the same fiber volume content.

(2) The residual strengths of 0° UD, 90° UD and 0°/90° specimens of this GFRP decrease fast in the early stage and then trend to be stable when moisture absorptions approach a saturate state. The dropping trends of residual tensile strengths of these three kinds of specimens correspond to the increment of their water absorption curves. The tensile strengths of all three kinds specimens have been reduced by more than 50% of the total declining quantity in the initial 20% of the aging time, and the tensile strength degradations of 0° UD, 90° UD and 0°/90° GFRP after 360 h hygrothermal aging are 8.37%, 30.33% and 14.38%, respectively. The tensile strength reduction rate of 90° UD GFRP is much more significant than that of 0° UD GFRP because its tensile strength is mainly dominated by the epoxy resin. Oppositely, the tensile strength of 0° UD GFRP is mainly dominated by glass fibers that are little affected by hygrothermal aging. This is reasonable that the strength retention rate of the orthogonal ply specimen falls in between those of specimens of 0° and 90° UDs.

(3) The proposed hygrothermal aging residual strength prediction models for UD represent inherent strength probabilities of fiber and matrix (fiber/matrix interface) phases in microscale. Additionally, they relate the hygrothermal aging of the tensile strength with the moisture concentration distribution through the Fickian diffusion theory. So they predict the strength reductions of epoxy resin matrix composites undergoing hygrothermal aging based on mechanism interpretation.

References

[1] MOURITZ A P, GELLERT E, BURCHILL P, et al. Review of advanced composite structures for naval ships and submarines[J]. Composite Structures, 2001, 53(1): 21-42.

[2] CHALMERS D W. The potential for the use of composite materials in marine structures[J]. Marine Structures, 1994, 7(5): 441-456.

[3] GÖKDENIZ N. Polymer based composites in marine use: history and future trends[J]. Procedia Engineering, 2017, 194: 19-24.

[4] BERKETIS K, TZETZIS D. Long-term water immersion ageing characteristics of GFRP composites [J]. Journal of Materials Science, 2009, 44(13): 3578-3588.

[5] LIAO K, SCHULTHEISZ C R, HUNSTON D L. Effects of environmental aging on the properties of pultruded GFRP[J]. Composites B, 1999, 30(5): 485-493.

[6] EFTEKHAR I, MOHAMMADREZ A, FATEM I, et al. Tensile behavior of thermoplastic composites including temperature, moisture, and hygrothermal effects [J]. Polymer Testing, 2016,51: 151-164.

[7] GUERMAZI N, BEN TARJEM A, KSOURI I, et al. On the durability of FRP composites for aircraft structures in hygrothermal conditioning[J]. Compos-

ites, 2016, 85: 294-304.

[8] ARUN K V, BASAVARAJAPPA S, SHERIGARA B S. Damage characterisation of glass/textile fabric polymer hybrid composites in sea water environment[J]. Materials & Design, 2010, 31(2): 930-939.

[9] RIAO L, LÉNAK B, CHAILAN J F, et al. Effect of interphase region on the elastic behavior of unidirectional glass-fiber/epoxy composites[J]. Composite Structures, 2018, 198: 109-116.

[10] ROY R, SARKAR B K, BOSE N R. Effects of moisture on the mechanical properties of glass fibre reinforced vinylester resin composites[J]. Bulletin of Materials Science, 2001, 24(1): 87-94.

[11] ASSARAR M, SCIDA D, MAHI A E, et al. Influence of water ageing on mechanical properties and damage events of two reinforced composite materials: Flax-fibres and glass-fibres[J]. Materials & Design, 2011, 32(2): 788-795.

[12] GARCIA E J D, CASTRO F D, GAYO P P, et al. Effects of sea water environment on glass fiber reinforced plastic materials used for marine civil engineering constructions [J]. Materials & Design, 2015, 66: 46-50.

[13] JOLIFF Y, REKIK W, BELEC L, et al. Study of the moisture/stress effects on glass fibre/epoxy composite and the impact of the interphase area[J]. Composite Structures, 2014, 108: 876-885.

[14] FIRDOSH S, NARASIMHA M H N, PAL R, et al. Durability of GFRP nanocomposites subjected to hygrothermal ageing[J]. Composites Part B Engineering, 2015, 69: 443-451.

[15] BELEC L, NGUYEN T H, NGUYEN D L, et al. Comparative effects of humid tropical weathering and artificial ageing on a model composite properties from nano- to macro-scale[J]. Composites Part A: Applied Science and Manufacturing, 2015, 68: 235-241.

[16] GELLERT E P, TURLEY D M. Seawater immersion ageing of glass-fibre reinforced polymer laminates for marine applications[J]. Composites Part A: Applied Science and Manufacturing, 1999, 30(11): 1259-1265.

[17] KAJORNCHEAPPUNNGAM S, GUPTA R K, GANGARAO H V S. Effect of aging environment on degradation of glass-reinforced epoxy[J]. Journal of Composites for Construction, 2002, 6(1): 61-69.

[18] TSENOGLOU C J, PAVLLDOU S, PAPASPYRIDES C D. Evaluation of interfacial relaxation due to water absorption in fiber-polymer composites[J]. Composites Science and Technology, 2006, 66(15): 2855-2864.

[19] MORALS A B D. Prediction of the longitudinal tensile strength of polymer matrix composites[J]. Composites Science & Technology, 2006, 66(15): 2990-2996.

[20] KOTANI M, YAMAMOTO Y, SHIBATA Y, et al. Strength prediction method for unidirectional GFRP after hydrothermal aging[J]. Advanced Composite Materials, 2011, 20(6): 519-535.

[21] PRITCHARD G, SPEAKE S D. The use of water absorption kinetic data to predict laminate property changes [J]. Composites, 1987, 18(3): 227-232.

[22] ZHANG B, YANG Z, SUN X, et al. A virtual experimental approach to estimate composite mechanical properties: Modeling with an explicit finite element method[J]. Computational Materials Science, 2010, 49(3): 645-651.

[23] YANG S L, LIU W Q, FANG Y, et al. Influence of hygrothermal aging on the durability and interfacial performance of pultruded glass fiber-reinforced polymer composites[J]. Journal of Materials Science, 2019, 54(3): 2102-2121.

[24] BULMANIS V N, GUNYAEV G M, KRIVONOS V V, et al. Atmospheric durability of polymer-fiber composites in cold climates[J]. Mechanics of Composite Materials, 1991, 27(6): 698-705.

[25] ASTM International. Test method for moisture absorption properties and equilibrium conditioning of polymer matrix composite materials: ASTM D5229/D5229M[S]. West Conshohocken, PA, USA: ASTM, 2014.

[26] ASTM International. Test method for tensile properties of polymer matrix composite materials: ASTM D3039/D3039M-14[S]. West Conshohocken, PA, USA: ASTM, 2014.

[27] SHEN C H, SPRINGER G S. Moisture absorption and desorption of composite materials[J]. Journal of Composite Materials, 1976, 10(1): 2-20.

[28] MASAHIR O, KOTAN I, YUSUK E, et al. Lifetime prediction of woven GFRP laminates under constant tensile loading in hydrothermal environment[J]. Mechanics of Time Dependent Materials, 2013, 17(2): 261-274.

[29] BERKETIS K, TZETZIS D. Long-term water immersion ageing characteristics of GFRP composites[J]. Journal of Materials Science, 2009, 44(13): 3578-3588.

[30] VALENTIN D, PARAY F, GUETTA B. The hygrothermal behaviour of glass fibre reinforced Pa66 composites: A study of the effect of water absorption on their mechanical properties[J]. Journal of Materials Science, 1987, 22(1): 46-56.

[31] WEIBULL W. A statistical distribution function of wide applicability[J]. Journal of Applied Mechanics, 1951, 18: 293-297.

[32] MAHESH S, PHOENIX S L, BEYERLEIN I J. Strength distributions and size effects for 2D and 3D composites with Weibull fibers in an elastic matrix[J]. International Journal of Fracture, 2002, 115(1): 41-85.

[33] GAO Z, REIFSNIDER K L, CARMAN G. Strength prediction and optimization of composites with statistical fiber flaw distributions[J]. Journal of Composite Materials, 1992, 26(11): 1678-1705.

[34] SHIH G C, EBERT L J. Theoretical modelling of the effect of the interfacial shear strength on the longitudinal tensile strength of unidirectional composites[J]. Journal of Composite Materials, 1987, 21(3): 207-224.

[35] MORAIS A B D. Stress distribution along broken fibres in polymer-matrix composites[J]. Composites Science & Technology, 2001, 61(11): 1571-1580.

[36] NORIHIKO T, KUNIHIRO T, HIROYUKI K. Evaluation of the mechanical properties of PMC interface using slice compression test—Analysis of transfer mechanism of interfacial shear stress[J]. Composite Interfaces Proceedings, 2000, 7: 349-361.

[37] DOTSENKO A M, POLYAKOV A N. Analytical description of the stress distribution in a specimen with a central hole[J]. Strength of Materials, 1989, 21(12): 1699-1703.

[38] LIU K, PIGGOTT M R. Fracture failure processes in polymers Ⅰ: Mechanical tests and results[J]. Polymer Engineering & Science, 1998, 38: 60-68.

[39] LIU K, PIGGOTT M R. Fracture failure processes in polymers Ⅱ: Fractographic evidence[J]. Polymer Engineering & Science, 1998, 38: 69-78.

Acknowledgements This work was supported by the National Natural Science Foundation of China (No.11872205), the State Key Laboratory Open Fund (No. MCMS-E-0221Y02), and the Priority Academic Program Development of Jiangsu Higher Education Institutions.

Authors Dr. **GAO Chaogan** received the Ph.D. degree in engineering mechanics from Nanjing University of Aeronautics and Astronautics (NUAA), China, in 2020. His current research interests mainly focus on the fracture, fatigue, damage and environmental aging of composites.

Prof. **ZHOU Chuwei** received his Ph.D. degree in Department of Solid Mechanics, Tsinghua University, Beijing, China, in 1999. Now he is a professor at College of Aerospace Engineering, NUAA. His current research interests include mechanical properties of laminated or textile composites, meso/micro-mechanics, and computational mechanics.

Author contributions Dr. **GAO Chaogan** designed the study, complied the models, and wrote the manuscript. Prof. **ZHOU Chuwei** contributed to the discussion and revision of the study. All authors commented on the manuscript draft and approved the submission.

Competing interests The authors declare no competing interests.

(Production Editor: ZHANG Huangqun)

GFRP湿致拉伸强度老化的细观力学研究

高超干，周储伟

(南京航空航天大学机械结构力学与控制国家重点实验室，南京 210016，中国)

摘要：研究了湿热老化对环氧树脂基复合材料拉伸强度的影响。首先进行了玻璃纤维增强聚合物(Glass fiber reinforced polymer, GFRP)的吸水性和湿致拉伸强度退化试验，试验结果显示该GFRP的吸湿行为符合Fick定律，其抗拉强度在湿热老化早期显著降低，然后逐渐平缓。然后，提出了单向纤维增强复合材料细观尺度纵向和横向强度预测模型，以反映纤维和基体(或纤维/基体界面)失效的固有概率以及吸湿率的影响。该模型可以预测环氧树脂基复合材料在不同湿热老化时间下的拉伸强度退化情况，并通过老化试验验证了模型的正确性。

关键词：复合材料；湿热老化；剩余强度；细观力学；概率模型